HEAT TREATMENT EFFECTS ON THE REDUCTION OF HYDROGEN IN MULTI-LAYER HIGH-STRENGTH WELD JOINTS

T. Mente, Th. Boellinghaus and M. Schmitz-Niederau

ABSTRACT

High-strength structural steels with yield strengths up to 1 100 MPa are used in various industrial sectors such as for the construction of cranes, pipelines and offshore structures. However, with increasing strength the ductility and deformation capacities of these materials are reduced and thus, they show an enhanced sensitivity against degradation due to hydrogen with increasing yield strength. It means they become susceptible to hydrogen-assisted cold cracking (HACC) during fabrication welding. In order to avoid such defects, the existing standards recommend preheating and/or interpass temperature, as well as post heat treatments. However, the standards relate only to steels with a maximum yield strength of $R_{p0.2}$ = 960 MPa. Hence, in welding these high-strength structural steels with yield strengths up to 1 100 MPa, it is very important to have practical guidelines for determining suitable heat treatment procedures to avoid HACC in welds, in particular in safety-relevant components. As a contribution to the further establishment of sufficient Hydrogen-Removal Heat Treatments (HRHT), two dimensional numerical models of butt and lap joints of various thicknesses were developed. Hydrogen diffusion and the effect of different post heat treatments upon hydrogen reduction in high-strength structural steel were studied. It turned out that the hydrogen diffusion behaviour in the lap and the butt joints are quite different and that the hydrogen concentration in the lap joint can be reduced significantly faster in comparison to the butt joint.

IIW-Thesaurus keywords: Cold cracking; Heat treatment; High strength steels; Hydrogen; Numerical simulation; Structural steels.

1 Introduction

The strength requirements of steels strongly increased during the last 20 years. Due to the rising demand for steels having a high strength in combination with sufficient ductility, high-strength structural steels were developed with yield strengths up to 1 300 MPa. Especially in fabrication of crane structural steels with yield strength of 1 100 MPa are applied [1] in order to improve the economy.

Achieving the respective high strength, the microstructure of those fine grained steels is complexly adjusted by means of alloying elements and thermal treatments. Due to their low carbon content high-strength structural steels have a good weldability. Nevertheless, the use of these modern high-strength steels was associated with spectacular failure cases [2]. Because, with increasing yield strength they show an enhanced sensitivity against degradation due to hydrogen and the ductility and deformation capacities of these materials are reduced.

As can be seen in Figure 1 the specific hydrogen concentration at which the tensile strength coincides with the 0.2 % proof stress decreases to lower values at higher strength classification level. These hydrogen concentrations represent significant values for the effects of hydrogen in limiting the ductility of a material to nearly zero. For all microstructures of the welded S1100, the limiting hydrogen concentration ranges at approximately 1.8 ml/100 g.

Historically, the risk of hydrogen-assisted cracking has been the greatest in the heat-affected zone, due to the susceptible microstructure as a result of the rapid cooling during the welding thermal cycle. Modern high-strength steels with yield strengths up to 1 100 MPa tend to form hydrogen-assisted cracks in the weld metal [4, 5], because the strength ratio between base material and filler material decreases and higher stress levels are reached in the matching or undermatching weld metal. Thus, lower levels of hydrogen will cause cracking in the weld metal rather than in the heat-affected zone.

High-strength structural steels possibly form hydrogen-assisted cold cracking (HACC) during manufacturing or hydrogen-assisted stress corrosion cracking (HASCC) during service operation.

Doc. IIW-2184, recommended for publication by Commission IX "Behaviour of Metals Subjected to Welding.

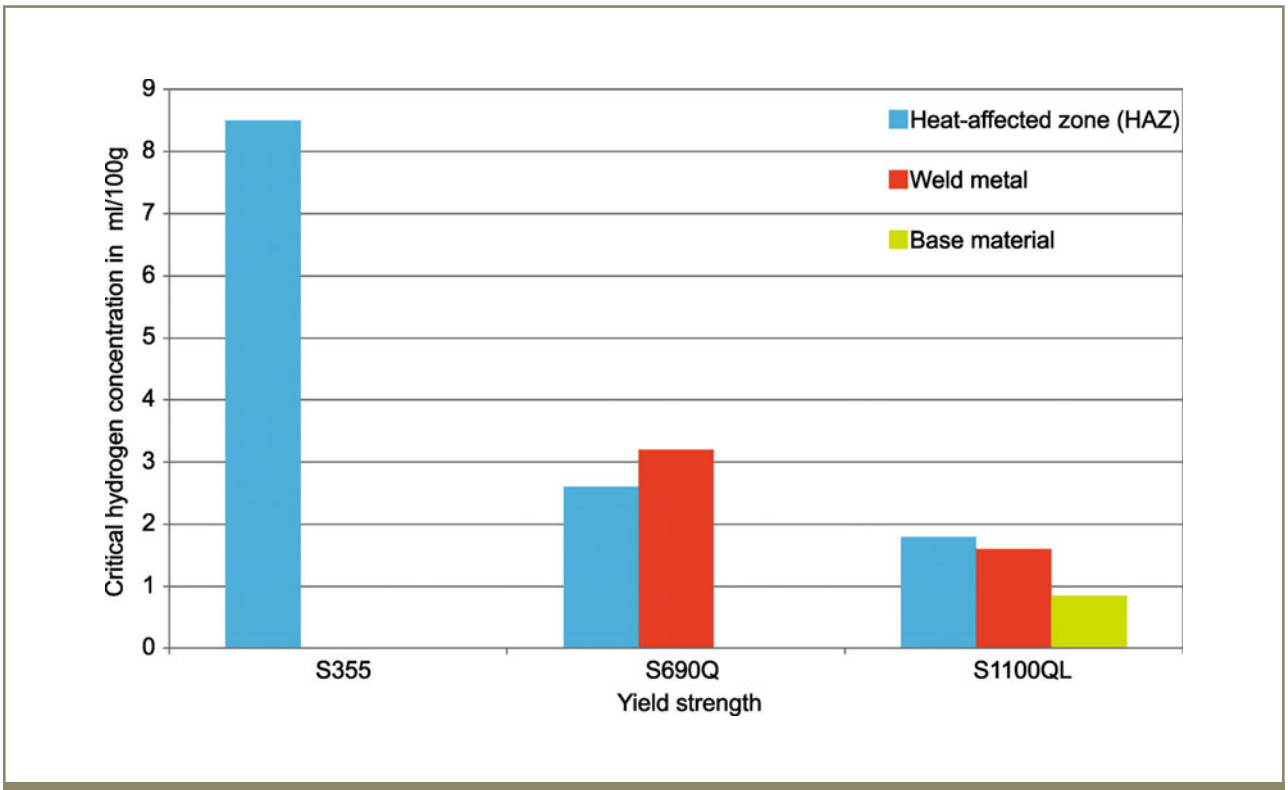

Figure 1 – Critical hydrogen concentration for which the tensile strength ranges at the level of the 0.2 % proof stress dependent on the strength classification level of the structural steels S355, S690 and S1100 [3]

Avoiding such damage, the existing standards recommend heat treatment procedures in order to lower the amount of introduced hydrogen. Two of these standards are AWS D1.1 and EN 1011-1 [6, 7], where preheating, interpass temperatures and post heating, respectively, is recommended as dehydrogenation heat treatment (DHT). But, only steels with minimum yield strengths up to 960 MPa are standardized in these standards, based on findings gained with materials of significantly lower strengths.

Previous studies of the effect of heat treatment procedures on the cold cracking behaviour of high-strength steels [8] showed that HACC can only be avoided if a dehydrogenation heat treatment procedure is applied that sufficiently reduces the hydrogen concentration.

In welding of high-strength structural steels with yield strengths of up to 1 100 MPa, it is very important to have practical guidelines to determine suitable heat treatment procedures avoiding HACC in welds, in particular for safety-relevant components. As a first step in this direction and contribution to further establishment of sufficient heat treatment procedures, some two-dimensional numerical models of butt and lap joints of different plate thickness were developed. The results are represented in so-called hydrogen removal heat treatment (HRHT) diagrams. Using these diagrams it is easy to determine appropriate dehydrogenation heat treatment temperatures and times avoiding hydrogen-assisted cold cracking in high-strength steels.

2 Numerical procedure

In the past, numerical methods were used in welding research and development. Today, the finite element method is increasingly applied in industry, since it can save time to perform parameter variations and the resulting effects can be extracted faster. Existing models can easily be transferred to other materials and structures and thus help saving time and effort. For simulating the hydrogen diffusion and the effect of DHT procedures on hydrogen reduction in butt and fillet welds, the commercial finite element program "ANSYS" was used. This software allows the input of appropriate simulation parameters via user-defined macros, written in the programming language "APDL" (ANSYS Parametric Design Language). The macros are saved as text file and can easily be modified in order to adjust parameters or change the geometry.

The simulation of hydrogen diffusion and DHT procedures is carried out in three indirect coupled stages [9], i.e. the result of the first step serves as basis for further calculations. The temperature field evaluated in the first step is used to calculate the temperature and microstructure dependent diffusion coefficients in the second step. Those are used in the third step simulating the hydrogen distribution in the welded joint.

In order to perform the numerical simulation, a base material with a yield strength of 1 100 MPa and a filler material according to AWS A5.28 [10] were chosen. The

Table 1 – Chemical compositions of materials used [max. wt. %]

	Fe	C	Si	Mn	Cr	Mo	Ni
Base material (Supplier - datasheet)	Bal.	0.18	0.50	1.30	1.50	0.70	2.50
Filler material AWS A5.28: ER 120S-G	Bal.	0.12	0.80	1.90	0.45	0.55	2.35

Table 2 – Mechanical properties of materials used

	Tensile strength [MPa] (ksi)	Yield strength [MPa] (ksi)	Minimum elongation A_5 ($A_{2\,in.}$) [%]
Base material (Supplier - datasheet)	1 200–1 500 (174–218)	1 100 (160)	10 (11)
Filler material AWS A5.28: ER 120S-G	830 (120)	n.s.	n.s.

n.s. – not specified.

corresponding chemical compositions and mechanical properties taken from the datasheets [11, 12] of the supplier are listed in Table 1 and Table 2. The welded joint is an undermatching connection, because as yet there are no filler materials available for steels having yield strengths up to 1 100 MPa. In order to make a statement about the effect of DHT on hydrogen reduction in the welded joint, more precise material properties following Wongpanya [13] were used in the numerical simulation for all welded microstructures. Thus, the results are applicable for both the weld metal and the heat-affected zone.

Two-dimensional models of butt and filled welds (Figure 2), each of a thickness of 6 mm, 12 mm and 20 mm, were constructed and used to perform the numerical simulation. All welded joints, except the 6 mm fillet weld, were multi-layer welds. For example, the 12 mm fillet weld in Figure 2 consists of three welding passes and the 12 mm butt weld of five welding passes according to [14]. The models were finely meshed at regions with high gradients as they occur in the weld. However, the number of elements was limited to 8 000 in the 20 mm fillet weld and to 5 200 in the 20 mm butt weld in order to minimize the computational effort. The numbers of elements is still adequate to achieve good results.

In the first step, the transient temperature field was calculated using temperature dependent material properties according to the diagrams given by Richter [15] for steels with similar chemical composition. The applied process parameters of a GMAW process with an energy input of 1.1 kJ/mm were adopted from previous studies [5, 14].

The simulation of the thermal cycle during welding was performed by setting the nodes of the respective layer to a homogeneous temperature above the melting point (≥ 1 540 °C) for three seconds [14, 16]. The welding time of three seconds includes an ascending time of one second in order to account for the torch travel through the respective cross-section. The filler material deposition was simulated using the element birth and death method of the FE-program "ANSYS". The DHT process was incorporated into the numerical simulation of multi-pass welds by assigning the respective temperature to those nodes

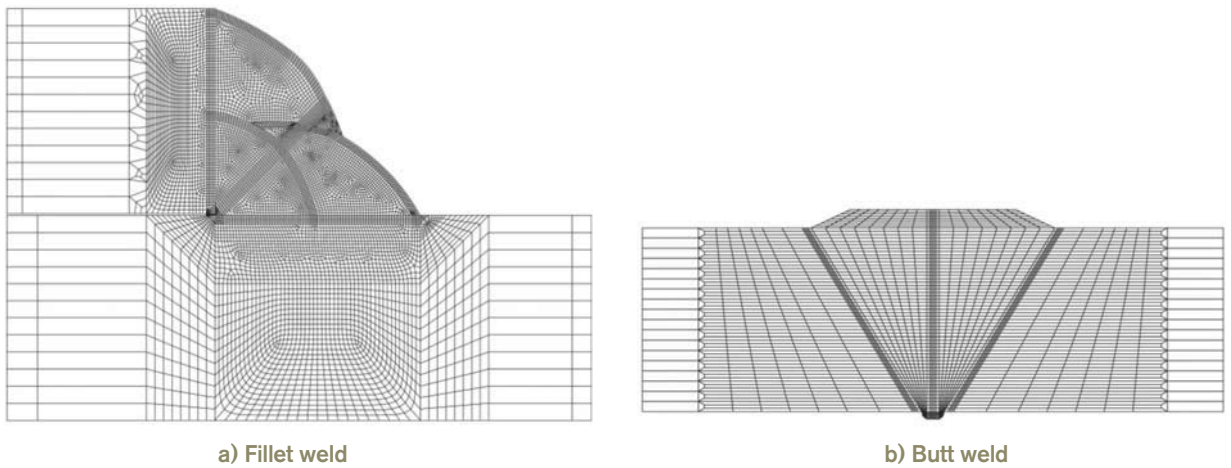

a) Fillet weld b) Butt weld

Figure 2 – Schematic illustration of the numerical models

on the surface where the heating pads were located for the specific time. After each layer and after DHT the model was allowed to cool down to room temperature at free heat convection and heat conduction by applying a surface film coefficient to all free surfaces of the model. Cooling down to room temperature after each layer takes 15 to 25 min depending on the joint configuration and plate thickness.

The calculated temperature field was used to determine the temperature, time and microstructure dependent diffusion coefficient. This was accomplished by using the Arrhenius relationship which reflects the strong temperature dependency of the diffusion coefficient:

$$D_{eff} = D_0 \cdot e^{-\frac{\Delta H}{RT}} \quad (1)$$

where

D_{eff} is the effective diffusion coefficient,

D_0 is the diffusion coefficient in normal state,

ΔH is the activation energy for hydrogen diffusion,

R is the universal gas constant and

T is the absolute temperature.

In determining the diffusion coefficients, it is important to use the same time step size as in the simulation of the temperature field. The diffusion coefficients were calculated for every time step and respective weld microstructure based on the equations of hydrogen diffusion coefficients in low alloyed carbon structural steels [17], as represented in Figure 3. These values cover the whole temperature range from room temperature to molten liquid temperature, as required for numerical simulation of hydrogen diffusion and effusion of low alloyed structural steel welds. Moreover, these diffusion coefficients consider the phase transformation during heating and cooling. Boellinghaus [18] experimentally showed that the real diffusion coefficient rather follows the upper envelope curve.

In order to obtain reliable DHT process values for HACC avoidance, all diffusion inhibiting effects have to be considered. A worst case assessment was simulated using the lower envelope.

In the third step, the determined diffusion coefficients were used to simulate the hydrogen diffusion based on the analogy of Fourier's heat conduction differential equation, Equation (2), and Fick's second law, Equation (3).

$$\rho \cdot c_p \left(\frac{\partial \vartheta}{\partial t}\right) = \left(\frac{\partial}{\partial x}\lambda\frac{\partial \vartheta}{\partial x} + \frac{\partial}{\partial y}\lambda\frac{\partial \vartheta}{\partial y}\right) + \dot{q}_E \quad (2)$$

$$\left(\frac{\partial HD}{\partial t}\right) = \left(\frac{\partial}{\partial x}D_{eff}\frac{\partial HD}{\partial x} + \frac{\partial}{\partial y}D_{eff}\frac{\partial HD}{\partial y}\right) \quad (3)$$

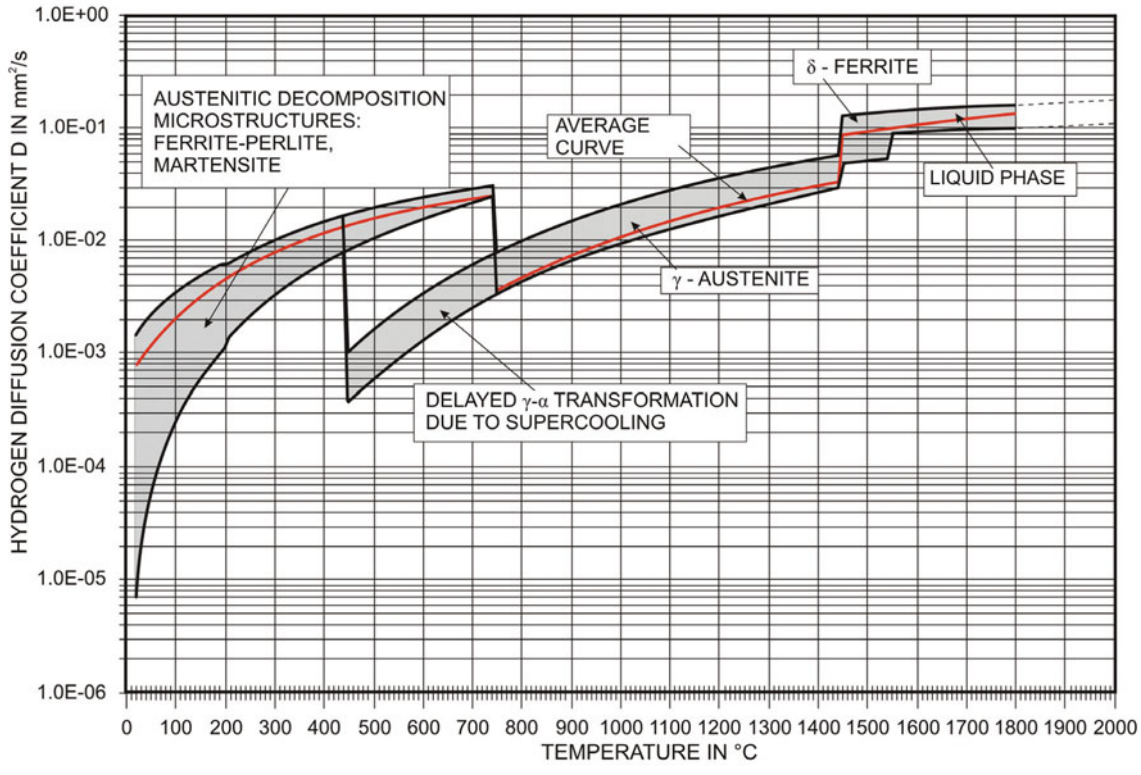

Figure 3 – Scatterband for hydrogen diffusion coefficients in low alloyed carbon structural steels [17]

Assuming that there is no heat source or sink ($\dot{q}_E = 0$) and replacing the temperature ϑ with the hydrogen concentration HD, the thermal conductivity λ with the effective diffusion coefficient D_{eff}, as well as equalizing the density ρ and the specific heat capacity c_p to one, hydrogen diffusion can be simulated using the thermal module in the finite element program "ANSYS". Therefore, the previously determined and externally saved diffusion coefficients were imported for every time step and applied to the corresponding element in the finite element model.

Hydrogen transfer in the weld metal was simulated via a Dirichlet boundary condition setting an initial hydrogen concentration of $HD_0 = 5$ ml/100 g to the corresponding nodes of the actual welded layer as long as the weld metal is molten. A homogeneous distribution of hydrogen was assumed. During cooling to room temperature, diffusion controlled hydrogen effusion was considered setting the hydrogen concentration at the surface to zero and removing the boundary condition from the weld. An initial hydrogen concentration of 5 ml/100 g was chosen to assure comparability to previous studies [13] according to the value for extra-low hydrogen consumables specified in the standards AWS D1.1 and EN 1011-1 [6, 7]. The base material was assumed to be free from hydrogen. The influence of stresses and strains on the hydrogen diffusion and distribution was neglected for all simulations to reduce the effort of the numerical simulations. In order to avoid hydrogen-assisted cracking, it is essential to consider the hydrogen distribution and the stresses and strains arising immediately after completion of the welding process at room temperature. Accumulation of hydrogen in highly-stressed areas of the weld takes a lot of time, as for example accumulation in front of a crack tip takes more than 20 days as shown by Olden *et al.* [19].

For determining heat treatment procedures with sufficient dehydrogenation, the temperatures were systematically varied from 50 °C to 250 °C in steps of 50 °C. The temperatures were limited to 250 °C, because it is known that higher temperatures cause annealing effects reducing the strength of the material [20]. The criterion for a heat treatment with sufficient dehydrogenation was determined by specifying reduced hydrogen concentration values of less than 1.8 ml/100 g. Zimmer *et al.* [3] mentioned that high-strength steels with yield strengths up to 1 100 MPa have no ductility at hydrogen concentration levels below this specified limit. The reduction of hydrogen below this limit does not provide a crack-free weld; even at lower hydrogen concentrations an overloading of the construction can occur.

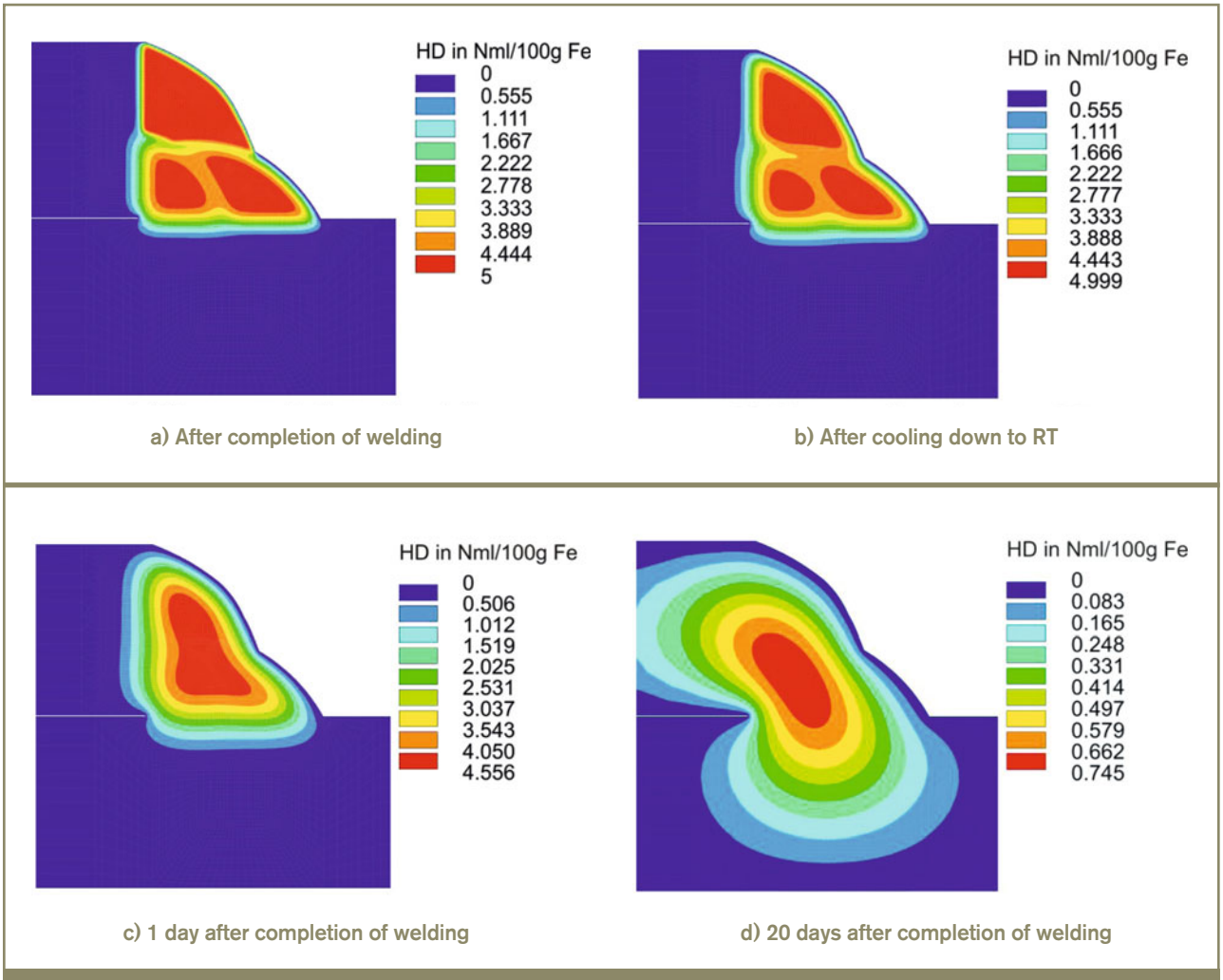

a) After completion of welding

b) After cooling down to RT

c) 1 day after completion of welding

d) 20 days after completion of welding

Figure 4 – Simulated hydrogen distribution in fillet weld at different times

For these reasons it should be noted that the determined Hydrogen-Removal Heat Treatment does not guarantee cold-crack-free welds of the steels used here. Those hydrogen removal heat treatments may be understood as a recommendation to exclude the hydrogen as a possible cause for cracking during manufacturing of those materials.

3 Results of the numerical simulation of hydrogen diffusion

3.1 General hydrogen distribution in high-strength steel welds

In Figure 4 the simulated distribution of the maximum hydrogen concentration is shown for the 12 mm fillet weld. In order to study the pure hydrogen diffusion and effusion in welded joints of such high-strength steels without the effects of heat treatments, effusion of 20 days at room temperature was modelled. As can be seen, most of the hydrogen remains in the weld metal for a very long time and most of the hydrogen effuses at room temperature.

Even in case of welding, only a low amount of hydrogen effuses from each weld bead during subsequent cooling to room temperature, due to the worst case diffusion coefficient applied to the model. The hydrogen concentration of each layer is reduced by a maximum of five percent during welding and subsequent cooling to room temperature, depending on the joint configuration and plate thickness, as well as on the amount of deposited metal.

The distribution of the hydrogen concentration over time at different points in the welded joint is shown in Figure 5. It is seen that the hydrogen concentration in the first bead (point A, root weld) and in the second bead (point B) is slightly lower, due to reheating during manufacturing. By reheating the first and the second beads, the hydrogen can effuse at higher temperatures and thus diffuse into the hydrogen-free material to reach the surface to effuse. The longer diffusion path to the surface of the first bead, at which hydrogen can effuse, causes much more time to reduce hydrogen concentration than in the other weld beads.

The hydrogen concentration in the HAZ (points L, M and O) slightly increases to a maximum, due to a concentration gradient in the weld metal and in the heat-affected zone (HAZ). But, with increasing time, the gradient is reduced by the effusion of hydrogen and the hydrogen concentration in the HAZ decreases again. Nevertheless, crack critical values of hydrogen concentration are achieved.

The hydrogen diffusion in the butt weld is quite similar. The hydrogen concentration in the root weld is reduced much faster than in the root of the fillet weld, because the ratio of deposited weld metal to the free weld layer surface is smaller in the butt weld. The reasons for the overall faster hydrogen reduction in the butt weld are a larger heat quantity and slower cooling times. Hydrogen can effuse much longer at high temperatures, thus the hydrogen concentration in the middle of the weld is slightly lower than in the fillet weld after the weld is finished and less hydrogen has to be removed from the middle of the welded joint.

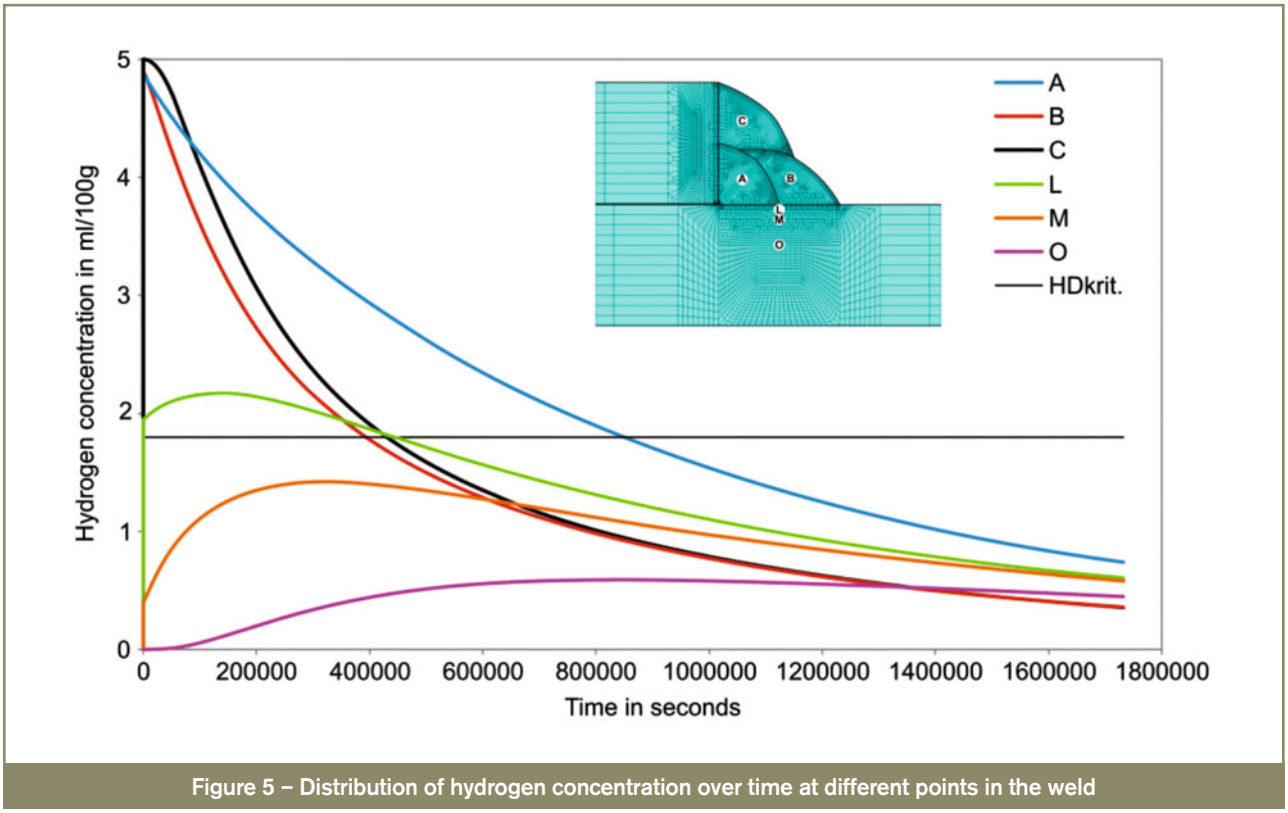

Figure 5 – Distribution of hydrogen concentration over time at different points in the weld

3.2 Hydrogen diffusion depending on manufacturing process

In addition to the effects of post heat treatments, manufacturing-related factors affecting the hydrogen diffusion were investigated. In this case, the impact of an increase in the number of weld beads at constant weld volume was studied. Therefore, the numerical model of the 12 mm fillet weld was used and the number of weld beads increased from three to six beads. Increasing the number of weld beads involves an increase in heat quantity, so hydrogen effuses faster (Figure 6). Due to the fact that the weld volume is the same, also the amount of hydrogen is the same. But, the diffusion path to the free surface is shorter during welding. Hence, the hydrogen concentration in the middle of the weld is slightly lower after the weld is finished and lower overall amounts of hydrogen have to be reduced.

As can be seen in Figure 6, the reduction of hydrogen at point C is very fast in the fillet weld made with six beads, because the point is closer to the surface than in the three bead fillet weld. This allows the hydrogen to effuse much faster from this point. The hydrogen concentration in the HAZ is only slightly different, as can be seen from the light green curves.

It can be said that an increase in the number of layers at constant weld volume has a favourable effect on the hydrogen reduction. But, the aspect of residual stresses has to be observed. As described in [21] residual stresses can be reduced in longitudinal direction by increasing the number of beads, which especially reduces the residual stresses in the root layer. But the transversal residual stresses increase, because at high restraint conditions, the hindering in shrinkage increases with the number of weld beads. The quantity of increased residual stresses and the influence of their interaction with lower hydrogen concentrations on the effect of cold cracking were not examined here.

However, even if the quantity of heat is higher in the six bead weld, the reduction of hydrogen after completion of welding is much faster in the butt weld, due to the slower cooling during welding.

3.3 Hydrogen diffusion depending on plate thickness

The plate thickness has a significant influence on the hydrogen diffusion in welded joints. Increasing the plate thickness involves an increase in the weld volume and thus, in the amount of introduced hydrogen. In contrast, the weld surface increases only slightly compared to the weld volume. Greater thickness means a longer diffusion path on which hydrogen must be transported to effuse at the free surface. In addition, thicker plates cool down even faster during manufacturing and reduce less the hydrogen concentration in the already welded layers.

The restraint intensity also increases with increasing plate thickness [22] leading to higher residual stresses and strains in the welded joint. Thereby, the risk of hydrogen-assisted cold cracking is increased.

Figure 7 shows the distribution of the maximum hydrogen concentration over time without any heat treatment in the butt (BW) and fillet welds (FW) of various thicknesses. The maximum hydrogen observed is the highest hydrogen concentration present in the welded joint at the respective

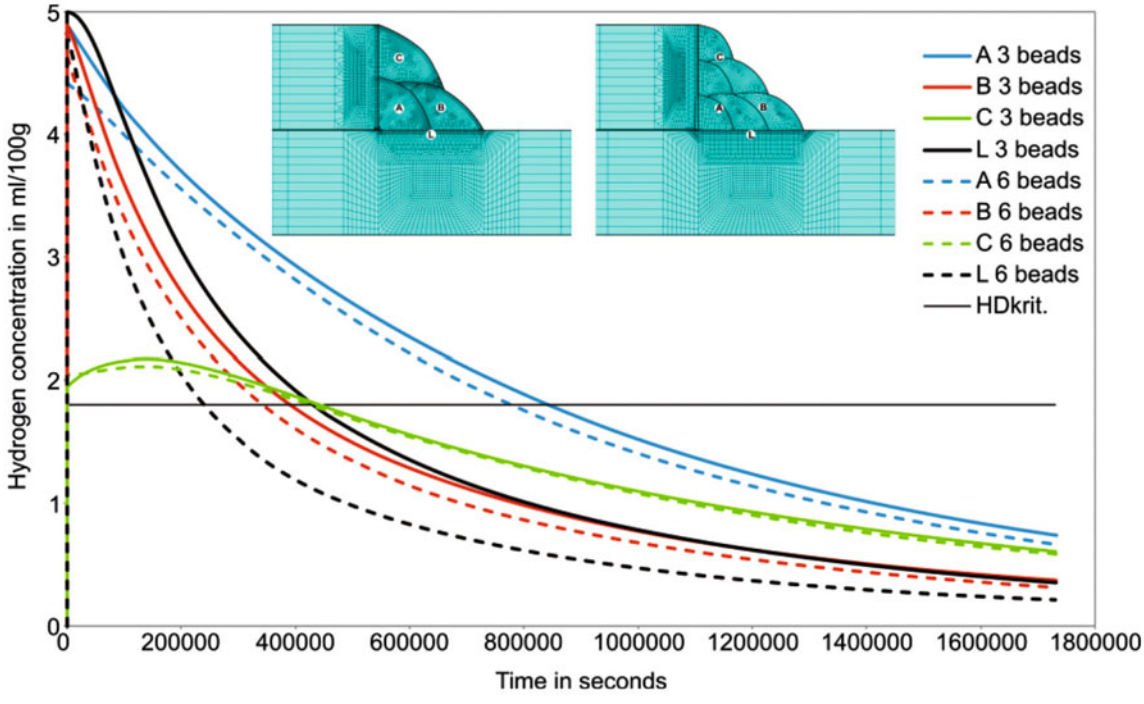

Figure 6 – Hydrogen diffusion with different numbers of weld beads (12 mm lap joint)

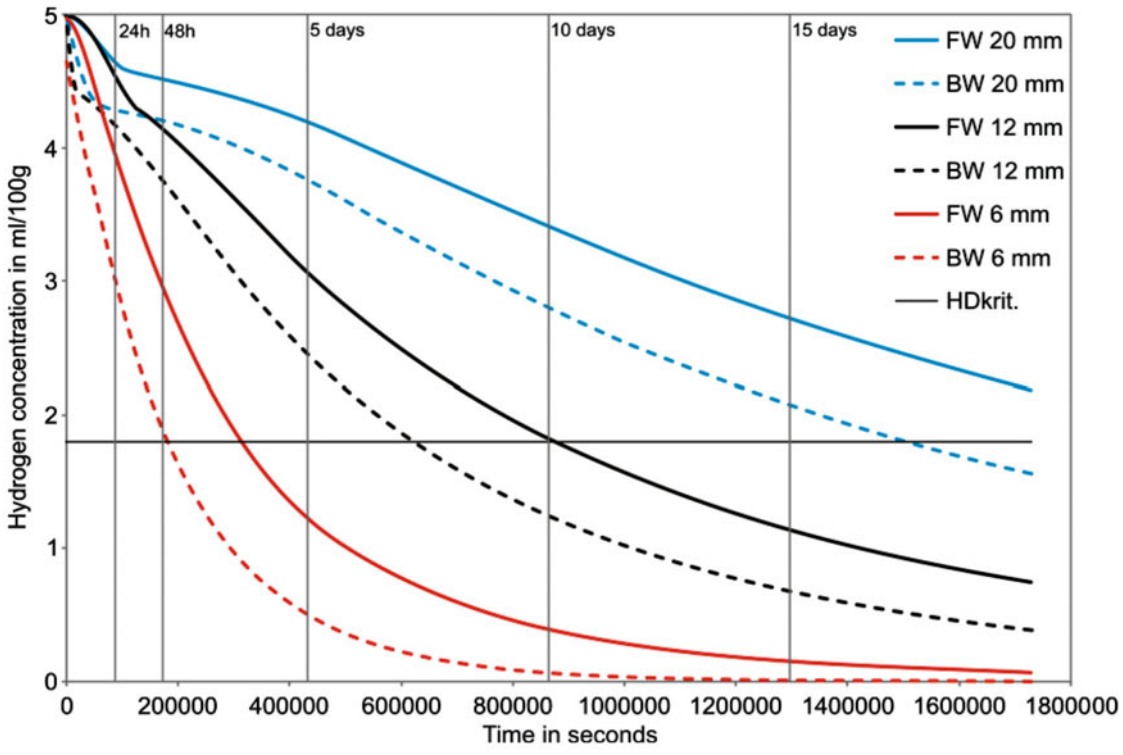

Figure 7 – Hydrogen diffusion in butt (BW) and fillet (FW) weld depending on plate thickness

time. The location of the maximum hydrogen concentration within the welded joint varies regarding the different joint configurations and plate thicknesses. As can be seen from the diagram, the hydrogen concentration is reduced much faster in the butt weld than in the fillet weld. The fillet weld cools down much faster during manufacturing, due to the larger volume of material. Therefore, the hydrogen in the root and in the intermediate layers can effuse much longer at higher temperatures in the butt weld and a lower amount of hydrogen in the middle of the weld has to be reduced after finishing welding.

The fast decay of the hydrogen concentration at the beginning of the curves, results from the position of the maximum hydrogen in the weld directly after welding. The maximum hydrogen concentration is located in the last layer, at short distance to the surface. At first, the maximum hydrogen concentration is reduced very fast and with increasing effusion time, the diffusion path grows longer and the gradient decreases.

The existing standards recommend at least 48 h waiting time before non-destructive testing [6] in order to detect delayed cracking. As can be seen in Figure 7, at this time there are still crack critical values of hydrogen concentration remaining in the welded joint. For example, the hydrogen concentration in the 12 mm fillet weld is reduced to only about 9 % of the initial hydrogen concentration of 5 ml/100 g. It takes more than ten days for the hydrogen concentration to drop to subcritical values without any heat treatments. As long as the hydrogen concentration is higher than $HD_{krit.}$ = 1.8 ml/100 g there is a drastically increased risk of hydrogen-assisted cracking. Therefore, marginal additional loads during service can easily cause cracking. Due to the very slow hydrogen effusion, it is very important to reduce the amount of hydrogen to a minimum. This can be achieved most effectively by applying an appropriate dehydrogenation heat treatment.

3.4 Effects of dehydrogenation heat treatments on hydrogen diffusion

Previous studies [8, 14, 23] relating to the effects of heat treatment procedures on the cold cracking behaviour of high-strength steels showed that only a sufficient dehydrogenation heat treatment can reduce the hydrogen concentration to a minimum decreasing the risk of HACC. These investigations also show that preheating at higher temperatures causes higher residual stresses. In addition, preheating shifts a higher amount of hydrogen into the crack critical HAZ. These higher amounts of hydrogen remain very long in the HAZ, if no additional dehydrogenation heat treatment is applied. In order to avoid HACC in welds of high-strength steels, all influencing effects on HACC have to be considered, namely the mechanical load, the hydrogen concentration and the microstructure.

Applying sufficient dehydrogenation heat treatment, hydrogen can quickly be reduced without increasing residual stresses. Indeed, the hydrogen concentration is also shifted into the crack critical HAZ, but decreases within minutes after reaching a maximum, as shown in Figure 8. For this

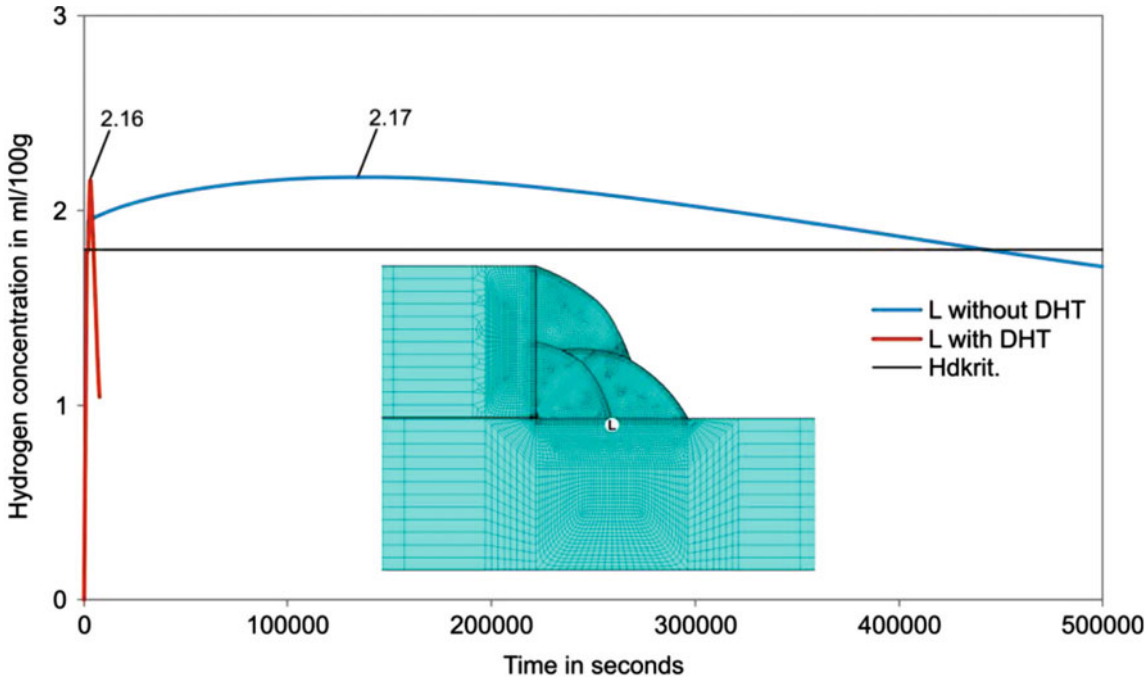

Figure 8 – Comparison of hydrogen diffusion in coarse HAZ with and without dehydrogenation heat treatment (DHT)

case the post heating temperature was 250 °C. In addition, no higher hydrogen concentrations were observed applying a dehydrogenation heat treatment. If no heat treatment is applied, it needs more than a few days until the hydrogen concentration has reached subcritical values.

In order to deduce practical guidelines from the simulated dehydrogenation heat treatment, the results have to be prepared and presented in Hydrogen-Removal Heat Treatment (HRHT) diagrams, as shown in Figure 9. These diagrams are normalized diagrams, determined from the results obtained by relating the actual hydrogen concentration present in the welded joint after DHT to the initial hydrogen concentration introduced during welding process.

Those normalized diagrams allow determining a sufficient DHT time and temperature for arbitrary initial concentrations. This description is possible, because there is a linear relationship between actual hydrogen concentration and initial concentration at a specific point for a specific time [24]. The reason for this linear relationship can be explained regarding the diffusion in an infinite half-space as the easiest solution of Fick's second law introducing the Gauss error function erf(z):

$$HD(x,t) = \frac{HD_0}{2}\left[1 - \mathrm{erf}\left(\frac{x}{2\sqrt{Dt}}\right)\right] \quad (4)$$

If the time t, the location x and the diffusion coefficient $D(x,y,z,t,\vartheta)$ are kept constant the term in the brackets will be a constant value and the hydrogen concentration HD(x,t) will depend linearly on the initial concentration HD_0.

For example, a reduction of hydrogen to subcritical values below 1.8 ml/100 g regarding an initial concentration of $HD_0 = 5$ ml/100 g means a reduction below 36 %. Thus, DHT of 240 min at 200 °C would be sufficient for the 12 mm butt weld and DHT of 240 min at 150 °C would be sufficient for the 12 mm fillet weld reducing the hydrogen concentration below the critical value of 1.8 ml/100 g.

For comparison of the hydrogen removal heat treatment behaviour in the butt and fillet welds, the curves of the 12 mm fillet and butt welds are plotted in Figure 9. It can be seen that the curves overlap with increasing temperature and time. Remembering Figure 7, the hydrogen concentration in the butt weld reduces much faster than in the fillet weld without any heat treatment. In the case of DHT these effects are reversed. Applying DHT a larger material volume is heated up to higher temperatures. Thus, the hydrogen can diffuse into the adjacent hydrogen-free material to reach the free surface. Furthermore, the ratio between the weld metal surface and the weld metal volume is much better in the fillet weld, due to the larger included angle. Also, the diffusion distance is shorter. Hydrogen has to be transported over a shorter diffusion distance, thus hydrogen concentration can be reduced much faster at a precipitous gradient. After a few minutes at higher DHT-temperatures the hydrogen concentration in the fillet weld is much lower than that in the butt weld.

Increasing the diffusion time at higher temperatures the concentration gradient decreases and the difference between the hydrogen concentration in the butt and fillet weld gets smaller.

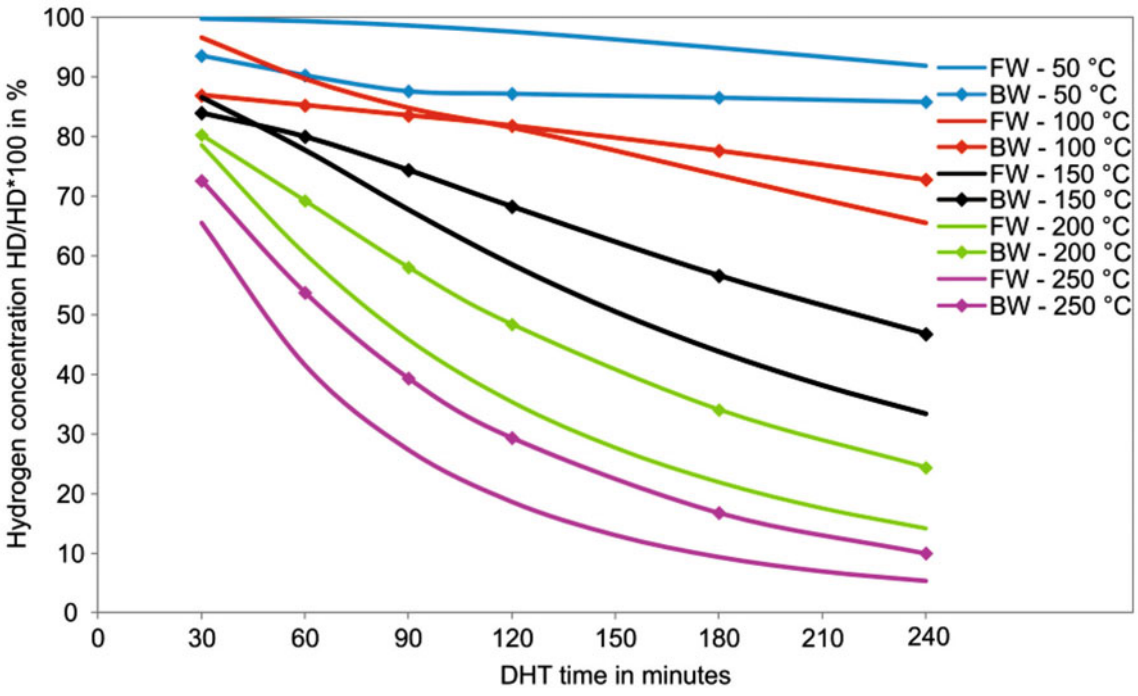

Figure 9 – Comparison of the HRHT curves between the 12 mm fillet (FW) weld and the 12 mm butt (BW) weld

Also, HRHT-curves for 6 mm and 20 mm welds were investigated, but are not shown here. It should be mentioned that the diffusion and effusion behaviour is the same as for the 12 mm welds. With increasing time and temperature the curves for the butt and fillet welds overlap. But, the hydrogen concentration in the 6 mm welds can be reduced much faster, while the reduction takes longer in the 20 mm welds, according to the diffusion behaviour shown in Figure 7. Thus, the HRHT diagram for a specific weld configuration is not transferable to other weld geometries and materials, due to the different diffusion behaviour.

4 Conclusions

1. It has been shown that a large amount of hydrogen primarily effuses at room temperature if a worst case diffusion coefficient is assumed and the risk of hydrogen-assisted cracking increases for a long time. Therefore, it is recommended to apply a dehydrogenation heat treatment (DHT) in order to minimize the hydrogen concentration avoiding hydrogen-assisted cracking, even at lower plate thickness.
2. Increasing the plate thickness prolongs the effusion time, due to the longer diffusion path to the free surface and to the higher amount of introduced hydrogen. In addition, the larger material volume causes faster cooling during the welding process, while less hydrogen can effuse at higher temperatures.
3. Without dehydrogenation heat treatment, hydrogen can be reduced much faster in butt welds compared to fillet welds. This may be due to the larger heat quantity and the somewhat slower cooling in the butt weld. However, if a dehydrogenation heat treatment is applied, hydrogen can be reduced faster in fillet welds, even at higher temperatures. The hydrogen can disperse into a larger hydrogen-free area to reach the surface where hydrogen can effuse. In addition, the hydrogen diffusion path is shorter in the fillet weld.
4. This opposite effect shows clearly that the temperature-dependent diffusion effects outweigh the geometry-dependent effects.
5. In general, the amount of introduced hydrogen can be reduced very quickly by DHT, without increasing the hydrogen concentration in crack critical HAZ regions. Moreover, residual stresses are not increased by DHT, as shown for sole preheating at higher temperatures [8].
6. With the help of numerical investigations of dehydrogenation heat treatment procedures, appropriate Hydrogen-Removal Heat Treatment diagrams can be determined very quickly for different materials, weld configurations and plate thicknesses. HRHT diagrams are very useful tools in practice to avoid hydrogen-assisted failure in high-strength steel welds.
7. In general, numerical simulations can help to formulate new standards for modern high-strength steel welding, also with a view to developing new filler metals.

References

[1] Goldež S., Knez M., Jezernik N. and Kramberger J.: Fatigue and fracture behaviour of high strength steel S1100Q, Engineering Failure Analysis, 2009, vol. 16, no. 7, pp. 2348-2356.

[2] Hagin B.: Project Cleuson-Dixence and the accident on Dec. 12th 2000, Proceedings on High Strength Steels for Hydropower Plants, 2005, Graz.

[3] Zimmer P., Boellinghaus Th. and Kannengiesser Th.: Effects of hydrogen on weld microstructure mechanical properties of the high strength steels S 690Q and S 1100QL, IIW Doc. II-1525-04, 2004.

[4] Nevasmaa P.: Prevention of weld metal hydrogen cracking in high-strength multipass welds, Doc. IIW-1617, Welding in the World, 2004, vol. 48, no. 5/6, pp. 2-18.

[5] Aström H., Nicholson F. and Wedberg F.: Consumables for welding high strength steels – Development and metallurgical problem areas, IIW Doc. II-1460-02, 2002.

[6] ANSI/AWS D1.1/D1.1M:2004: Structural Welding Code – Steel, American Welding Society.

[7] EN 1011-1:2009, Welding – Recommendations for welding of metallic materials – Part 1: General guidance for arc welding.

[8] Wongpanya P.: Effects of heat treatment procedures on the cold cracking behaviour of high strength steel welds, 2008, PhD-Thesis, Helmut Schmidt University – University of the Federal Armed Forces Hamburg, 281 pages.

[9] Lindgren L.-E.: Numerical modelling of welding, Computer methods in applied mechanics and engineering, 2006, vol. 195, no. 48-49, pp. 6710-6736.

[10] AWS A5.28/A5.28M:2005, Specification for low-alloy steel electrodes and rods for gas shielded arc welding, American Welding Society.

[11] Dillinger Hütte GTS: Dillimax 1100 – High strength fine grained structural steel quenched and tempered, Materials data sheet, February 2002, Specification DH-E55-B, Online: http://www.ancoferwaldram.nl/getdoc/78a40d5b-0d22-48df-a1ea-1eeb3cd5635d/dillimax1100-e.aspx

[12] SSAB Oxelösund: Weldox® 1100 – Data sheet, 2005, Online: http://www.ssab.com/Global/WELDOX/Datasheets/en/129_WELDOX_1100_UK_Data%20Sheet.pdf.

[13] Wongpanya P., Böllinghaus Th. and Lothongkum G.: Numerical simulation of hydrogen removal heat treatment procedures in high strength steel welds, Mathematical Modelling of Weld Phenomena 8, Cerjak H. (ed.), Verlag der Technischen Universität Graz, 2007, pp. 743-765, ISBN: 978-3-902465-69-6.

[14] Wongpanya P., Boellinghaus Th., Lothongkum G. and Kannengiesser Th.: Effects of preheating and interpass temperature on stresses in S 1100 QL multi-pass butt-welds, Doc. IIW-1851, Welding in the World, 2008, vol. 52, no. 3/4, pp. 79-92.

[15] Richter F.: Physikalische Eigenschaften von Stählen und ihre Temperaturabhängigkeit – Polynome und grafische Darstellungen, Physical properties of steels and their dependency on temperature – Polynoms and graphical presentation, Stahleisen-Sonderberichte, 1983, vol. 10, 42 pages (in German).

[16] Lindgren L.-E.: Finite element modeling and simulation of welding Part 1: Increased complexity, Journal of Thermal Stresses, 2001, vol. 24, no. 2, pp. 141-192.

[17] Boellinghaus Th., Hoffmeister H. and Dangeleit A.: A scatterband for hydrogen diffusion coefficients in micro-alloyed and low carbon structural steels, Doc. IIW-1250, Welding of the World, 1995, vol. 35, no. 2, pp. 83-96.

[18] Boellinghaus Th.: Zur Bestimmung risskritischer Schrumpfbehinderungen und Wasserstoffverteilungen in Schweißverbindungen durch numerische Simulation, Assignment of crack critical hindrance of shrinkage and the distribution of hydrogen in weld joints through numerical simulations, 1995, PhD-Thesis, Helmut Schmidt University – University of the Federal Armed Forces Hamburg, 204 pages (in German).

[19] Olden V., Thaulowa C., Johnsena R., Østbyb E. and Berstad T.: Application of hydrogen influenced cohesive laws in the prediction of hydrogen induced stress cracking in 25%Cr duplex stainless steel, Engineering Fracture Mechanics, 2008, vol. 75, no. 8, pp. 2333-2351.

[20] Bhadeshia H.K.D.H. and Honeycombe R.: Steels – Microstructure and Properties, Third Edition, Butterworth-Heinemann publications, Elsevier Ltd, ISBN: 978-0-750-68084-4, 2006, pp. 183-208.

[21] Macherauch E. and Hauk V.: Eigenspannungen: Entstehung-Messung-Bewertung, Residual stresses: development-measurement-quantification, Ed.: 1, Deutsche Gesellschaft für Metallkunde e.V., Oberursel, ISBN 3-88355-075-2, 1983 (In German).

[22] Boellinghaus Th., Kannengiesser Th. and Neuhaus M.: Effects of the structural restraint intensity on the stress strain build up in butt joints, Mathematical Modelling of Weld Phenomena 7, 2003, Verlag der Technischen Universität Graz, pp. 651-669, ISBN: 978-3901351990.

[23] Wongpanya P., Boellinghaus Th. and Lothongkum G.: Effects of hydrogen removal heat treatment on residual stresses in high strength structural steel welds, Welding in the World, 2006, vol. 50, Special Issue, pp. 96-103.

[24] Mehrer H.: Diffusion in solids – Fundamentals, methods, materials, diffusion-controlled process, Springer Series in Solid-State Sciences, 2007, vol. 155, Springer-Verlag Berlin Heidelberg New York, pp. 37-53, ISBN: 978-3-540-71486-6.

About the authors

Dipl. Ing. Tobias MENTE (tobias.mente@bam.de) and Prof. Dr.-Ing. Thomas BOELLINGHAUS (thomas.boellinghaus@bam.de) are with BAM Federal Institute for Materials Research and Testing, Berlin (Germany). Dr.-Ing. Martin SCHMITZ-NIEDERAU (Martin.Schmitz-Niederau@bsdg.de) is with Böhler Schweisstechnik Deutschland GmbH, Hamm (Germany).